Chapter 1
Smart Flat Ride Tuning

Hormoz Marzbani and Reza N. Jazar

Abstract Flat ride is the condition that the unpleasant pitch oscillation of the vehicle body turns into more tolerable bounce oscillation, when a car hits a bump in forward motion. Based on experimental results, Maurice Olley discovered and introduced two conditions for flat ride:

1. The radius of gyration in pitch should be equal to the multiplication of the distance from the mass centers a_1, a_2 of the front and rear wheels of the car ($r^2 = a_1 a_2$).
2. The rear suspension should have around 20% higher rate than the front. The equation $r^2 = a_1 a_2$ makes the car to be considered as two separated uncoupled mass-spring systems of front and rear suspensions.

In this chapter, we will analytically review the flat ride conditions and provide design charts to satisfy the required conditions. The nonlinear practical model of shock absorbers modifies the conditions which were based on linear models.

1.1 Flat Ride Definition

The excitation inputs from the road to a straight moving car will affect the front wheels first and then, with a time lag, the rear wheels. The general recommendation was that the natural frequency of the front suspension should be lower than that of the rear. So, the rear part oscillates faster to catch up with the front to eliminate pitch and put the car in bounce before the vibrations die out by damping. This is what Olley called the *flat ride tuning* [4]. Maurice Olley (1889–1983) established guidelines, back in the 1930, for designing vehicles with better ride. These were

H. Marzbani • R.N. Jazar (✉)
School of Aerospace, Mechanical and Manufacturing Engineering, RMIT University, Melbourne, VIC, Australia
e-mail: hormoz.marzbani@rmit.edu.au; reza.jazar@rmit.edu.au

R.N. Jazar and L. Dai (eds.), *Nonlinear Approaches in Engineering Applications 2*,
DOI 10.1007/978-1-4614-6877-6_1,

derived from experiments with a modified car to allow variation of the pitch mass moment. Although the measures of ride were strictly subjective, those guidelines are considered as valid rules of thumb even for modern cars. What is known as Olley's flat ride not considering the other prerequisites can be put forward as:

The front suspension should have around 30% *lower rate than the rear.*

An important prerequisite for flat ride was the uncoupling condition, which was introduced by Rowell and Guest for the first time in 1923 [4, 9]. Rowell and Guest used the geometry of a bicycle car model to find the condition which sets the bounce and pitch centers of the model located on the springs. Having the condition, the front and rear spring systems of the vehicle can be regarded as two separate one degree-of-freedom (DOF) systems.

In this study, using analytical methods, we study the flat ride conditions which have been respected and followed by the car manufacturers' designers since they were introduced for the first time. This article will provide a more reliable scientific and mathematical approach for what are the flat ride design criteria in vehicle dynamic studies.

1.2 Uncoupling the Car Bicycle Model

Consider the two DOF system in Fig. 1.1. A beam with mass m and mass moment I about the mass center C is sitting on two springs k_1 and k_2 to model a car in bounce and pitch motions. The translational coordinate x of C and the rotational coordinate θ are the usual generalized coordinates that we use to measure the kinematics of the beam. The equations of motion and the mode shapes are functions of the chosen coordinates.

The free vibration equations of motion of the system are:

$$\begin{bmatrix} m & 0 \\ 0 & I \end{bmatrix} \begin{bmatrix} \ddot{x} \\ \ddot{\theta} \end{bmatrix} + \begin{bmatrix} k_1 + k_2 & a_2k_2 - a_1k_1 \\ a_2k_2 - a_1k_1 & a_2^2k_2 + a_1^2k_1 \end{bmatrix} \begin{bmatrix} x \\ \theta \end{bmatrix} = 0 \tag{1.1}$$

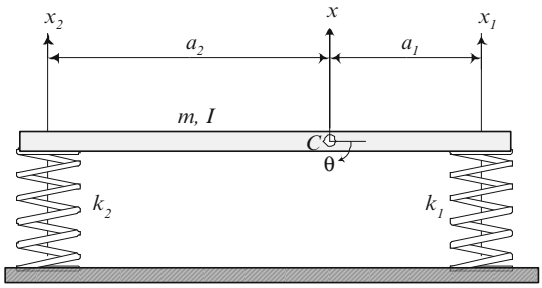

Fig. 1.1 The bicycle model of a car is a beam with mass m and mass moment I, sitting on two springs k_1 and k_2

To compare the mode shapes of the system practically, we employ the coordinates x_1 and x_2 instead of x and θ, as shown in Fig. 2.1. The equations of motion of the system would then be:

$$\begin{bmatrix} \frac{ma_2^2 + I}{a_1 + a_2{}^2} & \frac{ma_1a_2 - I}{a_1 + a_2{}^2} \\ \frac{ma_1a_2 - I}{a_1 + a_2{}^2} & \frac{ma_1^2 + I}{a_1 + a_2{}^2} \end{bmatrix} \begin{bmatrix} \ddot{x}_1 \\ \ddot{x}_2 \end{bmatrix} + \begin{bmatrix} k_1 & 0 \\ 0 & k_2 \end{bmatrix} \begin{bmatrix} x_1 \\ x_2 \end{bmatrix} = 0 \tag{1.2}$$

Let us define the following parameters:

$$I = mr^2 \tag{1.3}$$

$$\Omega_1^2 = \frac{k_1}{m}\beta \tag{1.4}$$

$$\Omega_2^2 = \frac{k_2}{m}\beta \tag{1.5}$$

$$\beta = \frac{l^2}{a_1 a_2} \tag{1.6}$$

$$\alpha = \frac{r^2}{a_1 a_2} \tag{1.7}$$

$$\gamma = \frac{a_2}{a_1} \tag{1.8}$$

$$l = a_1 + a_2 \tag{1.9}$$

and rewrite the equations as

$$\begin{bmatrix} \alpha + \gamma & 1 - \alpha \\ 1 - \alpha & \alpha + \frac{1}{\gamma} \end{bmatrix} \begin{bmatrix} \ddot{x}_1 \\ \ddot{x}_2 \end{bmatrix} + \begin{bmatrix} \Omega_1^2 & 0 \\ 0 & \Omega_2^2 \end{bmatrix} \begin{bmatrix} x_1 \\ x_2 \end{bmatrix} = 0 \tag{1.10}$$

Setting

$$\alpha = 1 \tag{1.11}$$

makes the equations decoupled

$$\begin{bmatrix} \alpha + \gamma & 0 \\ 0 & \alpha + \frac{1}{\gamma} \end{bmatrix} \begin{bmatrix} \ddot{x}_1 \\ \ddot{x}_2 \end{bmatrix} + \begin{bmatrix} \Omega_1^2 & 0 \\ 0 & \Omega_2^2 \end{bmatrix} \begin{bmatrix} x_1 \\ x_2 \end{bmatrix} = 0 \tag{1.12}$$

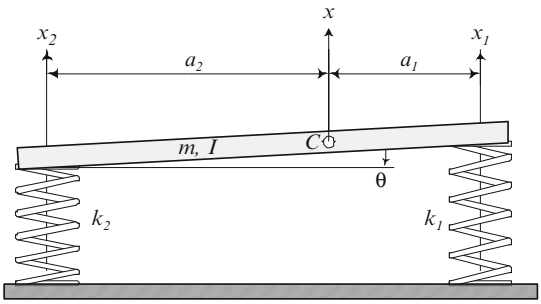

Fig. 1.2 The mode shape 1 for $\alpha = 1$ shows that only the front suspension is oscillating and the node is on the rear suspension

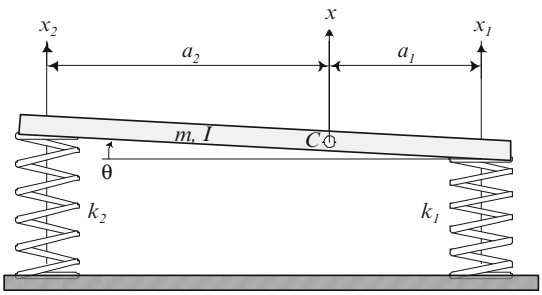

Fig. 1.3 The mode shape 2 for $\alpha = 1$ shows that only the rear suspension is oscillating and the node is on the front suspension

The natural frequencies ω_i and mode shapes u_i of the system are

$$\omega_1^2 = \frac{1}{\gamma + 1}\Omega_1^2 = \frac{l}{a_2}\frac{k_1}{m} \quad u_1 = \begin{bmatrix} 1 \\ 0 \end{bmatrix} \tag{1.13}$$

$$\omega_2^2 = \frac{\gamma}{\gamma + 1}\Omega_2^2 = \frac{l}{a_1}\frac{k_2}{m} \quad u_2 = \begin{bmatrix} 0 \\ 1 \end{bmatrix} \tag{1.14}$$

They show that the nodes of oscillation in the first and second modes are at the rear and front suspensions, respectively. Figures 1.2 and 1.3 illustrate the mode shapes of the bicycle car model for $\alpha = 1$.

The decoupling condition $\alpha = 1$ yields

$$r^2 = a_1 a_2 \tag{1.15}$$

which indicates that the pitch radius of gyration, r, must be equal to the multiplication of the distance of the mass center C from the front and rear axles. Therefore, by setting $\alpha = 1$, the nodes of the two modes of vibrations appear to be at the front and rear axles. As a result, the front wheel excitation will not alter the body at the rear axle and vice versa. For such a car, the front and rear parts of the car act independently. Therefore, the decoupling condition $\alpha = 1$ allows us to break

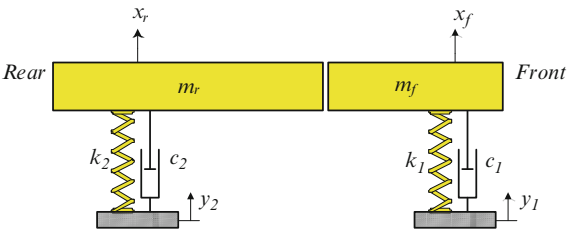

Fig. 1.4 Car bicycle model after decoupling

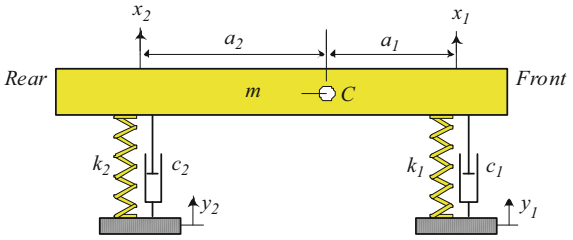

Fig. 1.5 Car bicycle model with damping

the initial two DOF system into two independent one DOF systems as illustrated in Fig. 1.4, where:

$$m_r = m\frac{a_1}{l} = m\varepsilon \tag{1.16}$$

$$m_f = m\frac{a_2}{l} = m(1-\varepsilon) \tag{1.17}$$

$$\varepsilon = \frac{a_1}{l} \tag{1.18}$$

The equations of motion of the independent systems will be:

$$m(1-\varepsilon)\ddot{x}_1 + c_1\dot{x}_1 + k_1x_1 = k_1y_1 + c_1\dot{y}_1 \tag{1.19}$$

$$m\varepsilon\ddot{x}_2 + c_2\dot{x}_2 + k_2x_2 = k_2y_2 + c_2\dot{y}_2 \tag{1.20}$$

The decoupling condition of undamped free system will not necessarily decouple the general damped system of Fig. 1.5. However, if there is no anti-pitch spring or anti-pitch damping between the front and rear suspensions, then equations of motion

$$\begin{bmatrix} \alpha+\gamma & 1-\alpha \\ 1-\alpha & \alpha+\frac{1}{\gamma} \end{bmatrix}\begin{bmatrix} \ddot{x}_1 \\ \ddot{x}_2 \end{bmatrix} + \begin{bmatrix} 2\xi_1\Omega_1 & 0 \\ 0 & 2\xi_2\Omega_2 \end{bmatrix}\begin{bmatrix} \dot{x}_1 \\ \dot{x}_2 \end{bmatrix} + \begin{bmatrix} \Omega_1^2 & 0 \\ 0 & \Omega_2^2 \end{bmatrix}\begin{bmatrix} x_1 \\ x_2 \end{bmatrix}$$
$$= \begin{bmatrix} 2\xi_1\Omega_1 & 0 \\ 0 & 2\xi_2\Omega_2 \end{bmatrix}\begin{bmatrix} \dot{y}_1 \\ \dot{y}_2 \end{bmatrix} + \begin{bmatrix} \Omega_1^2 & 0 \\ 0 & \Omega_2^2 \end{bmatrix}\begin{bmatrix} y_1 \\ y_2 \end{bmatrix} \tag{1.21}$$

$$2\xi_1\Omega_1 = \frac{c_1}{m}\beta \tag{1.22}$$

$$2\xi_2\Omega_2 = \frac{c_2}{m}\beta \tag{1.23}$$

will be decoupled by $\alpha = 1$

$$\begin{bmatrix} \alpha+\gamma & 0 \\ 0 & \alpha+\frac{1}{\gamma} \end{bmatrix} \begin{bmatrix} \ddot{x}_1 \\ \ddot{x}_2 \end{bmatrix} + \begin{bmatrix} c_1 & 0 \\ 0 & c_2 \end{bmatrix} \begin{bmatrix} \dot{x}_1 \\ \dot{x}_2 \end{bmatrix} + \begin{bmatrix} \Omega_1^2 & 0 \\ 0 & \Omega_2^2 \end{bmatrix} \begin{bmatrix} x_1 \\ x_2 \end{bmatrix}$$
$$= \begin{bmatrix} 2\xi_1\Omega_1 & 0 \\ 0 & 2\xi_2\Omega_2 \end{bmatrix} \begin{bmatrix} \dot{y}_1 \\ \dot{y}_2 \end{bmatrix} + \begin{bmatrix} \Omega_1^2 & 0 \\ 0 & \Omega_2^2 \end{bmatrix} \begin{bmatrix} y_1 \\ y_2 \end{bmatrix} \tag{1.24}$$

The equations of motion of the independent system of Fig. 1.4 may also be written as

$$m(1-\varepsilon)\ddot{x}_1 + c_1\dot{x}_1 + k_1x_1 = c_1\dot{y}_1 + k_1y_1 \tag{1.25}$$

$$m\varepsilon\ddot{x}_2 + c_2\dot{x}_2 + k_2x_2 = c_2\dot{y}_2 + k_2y_2 \tag{1.26}$$

which are consistent with the decoupled equations (1.24) because of

$$\varepsilon = \frac{1+\gamma}{\gamma\Omega_2^2} \tag{1.27}$$

To examine the effect of the decoupling condition and having independent front and rear model of a car, let us compare the responses of the model of Fig. 1.5 using (1.21) for different α.

Consider a car with the given characteristics in Table 1.1.

Table 1.1 Specification of a sample car

Specification	Nominalvalue
m (kg)	420
a_1 (m)	1.4
a_2 (m)	1.47
l (m)	2.87
k_1 (N/m)	10,000
k_2 (N/m)	13,000
c_1 (N s/m)	1,000
c_2 (N s/m)	1,000
β	4.00238
γ	1.05
Ω_1	95.2947
Ω_2	123.8832
ξ_1	0.05
ξ_2	0.0384

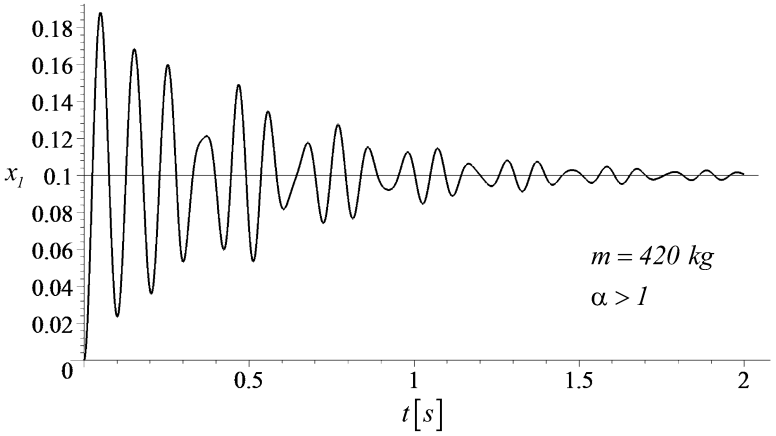

Fig. 1.6 Case 1: oscillations of the front of the car with $\alpha > 1$

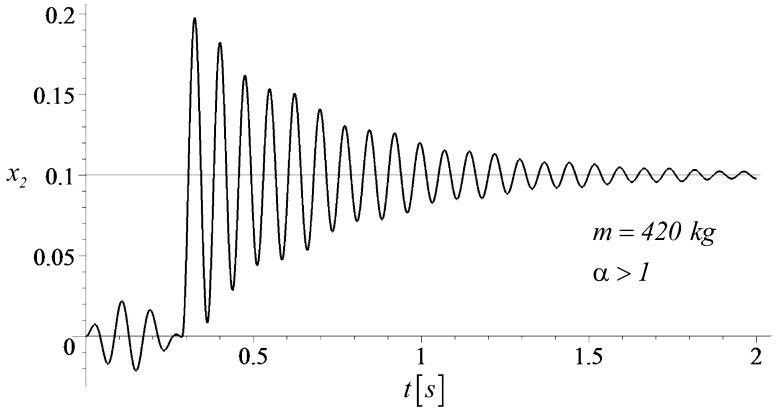

Fig. 1.7 Case 1: oscillations of the rear of the car with $\alpha > 1$

Figures 1.6–1.14 can be used for a comparison to show the effects of uncoupling the system when the car goes over a step

$$y_1 = 0.1\,\mathrm{m} \qquad y_1 = 0.1H\left(t - \frac{l}{v}\right)\,\mathrm{m} \tag{1.28}$$

where $H\,(x)$ is the Heaviside function

$$H\,(t-\tau) = \begin{cases} 0 & t \le \tau \\ 1 & t > \tau \end{cases} \tag{1.29}$$

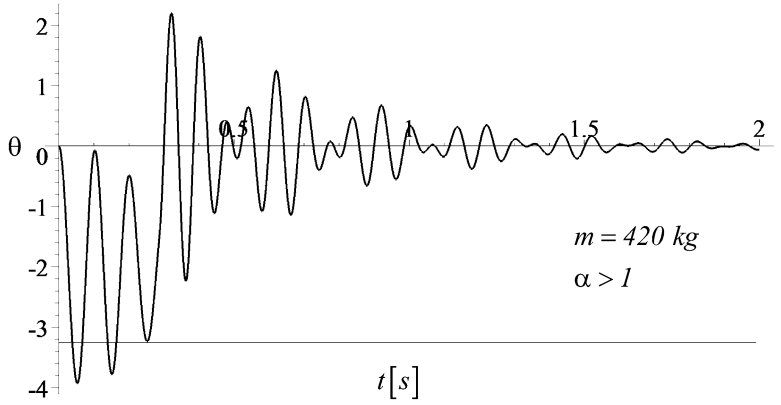

Fig. 1.8 Case 1: angular oscillations of the car with $\alpha > 1$

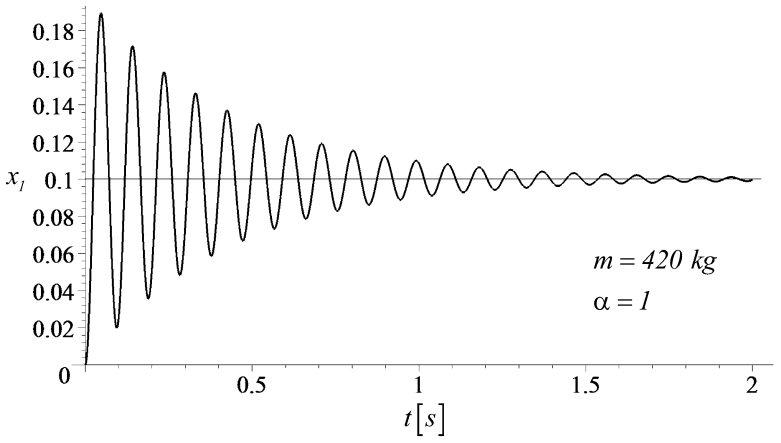

Fig. 1.9 Case 2: oscillations of the front of the car with $\alpha = 1$

Each set of three figures are for a value of α which varies from smaller than 1 to 1 and then bigger than 1.

- Case 1: $\alpha > 1$

$$\alpha = 1.2726\ ,\ r = 1.618\ ,\ I_y = 1100$$

- Case 2: $\alpha = 1$

$$\alpha = 1\ ,\ r = 1.434\ ,\ I_y = 864.36$$

- Case 3: $\alpha < 1$

$$\alpha = 0.8098 - r = 1.291 - I_y = 700$$

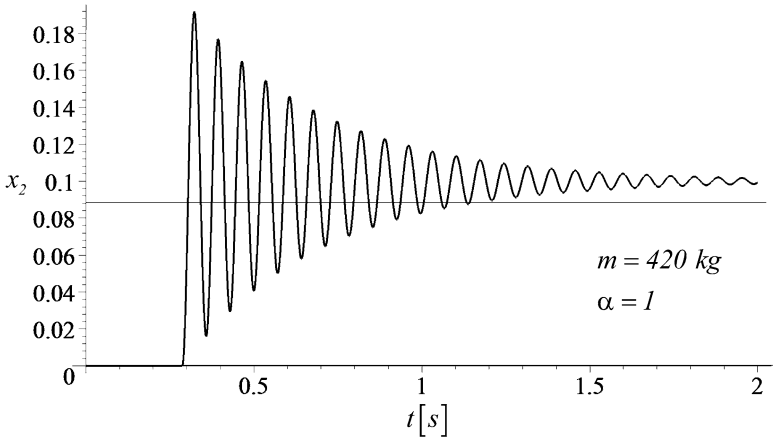

Fig. 1.10 Case 2: oscillations of the rear of the car with $\alpha = 1$

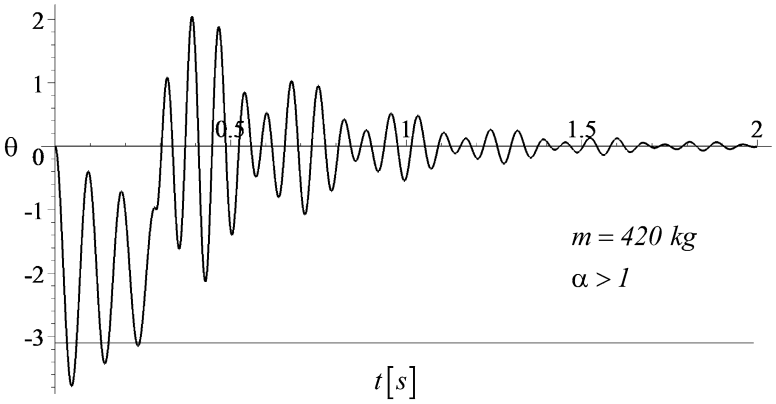

Fig. 1.11 Case 2: angular oscillations of the car with $\alpha = 1$

Figures 1.6–1.8 depict the oscillations of the front x_1, rear x_2, and pitch $\theta = (x_2 - x_1)/l$ for $\alpha = 1.2726 > 1$. Figures 1.9–1.11 show x_1, x_2, and θ for $\alpha = 1$, and Figs. 1.12–1.14 show x_1, x_2, and θ for $\alpha = 0.8098 < 1$.

Figures 1.6, 1.9, and 1.12 illustrate the oscillations of the front part of the vehicle after hitting the step for three different values of α. Similarly, Figs. 1.7, 1.10, and 1.13 illustrate the oscillations of the rear part of the vehicle after hitting the step for three different values of α. As it can be seen in Figs. 1.7 and 1.13 oscillations start with small amplitude, which does not exist in Fig. 1.10. The pitch vibrations behavior of the car for three different values of α can be compared in Figs. 1.8, 1.11, and 1.14.

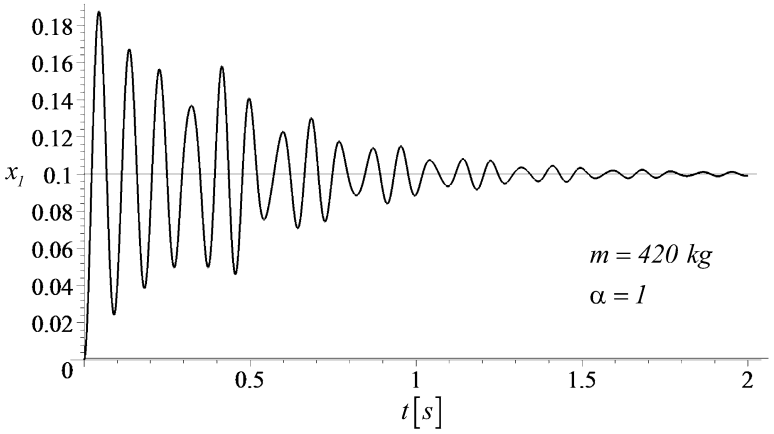

Fig. 1.12 Case 3: oscillations of the front of the car with $\alpha < 1$

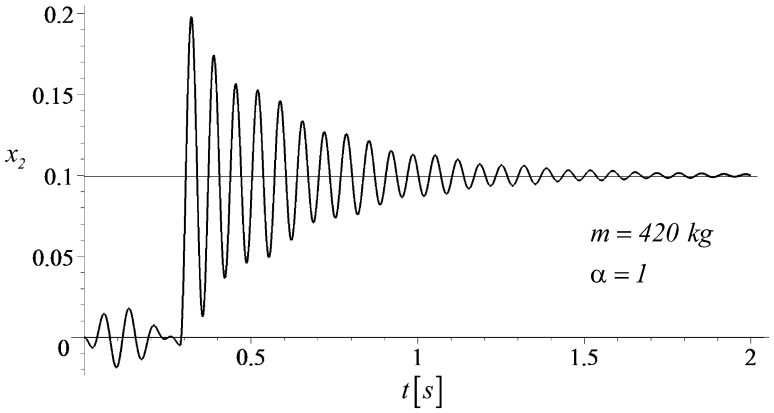

Fig. 1.13 Case 3: oscillations of the rear of the car with $\alpha < 1$

The delay in the oscillation of the rear of the vehicle is caused by the time lag between the front and the rear wheels hitting the step. This time lag is dependent to the wheelbase of the vehicle and also changes with the traveling speed shown by $\tau = \frac{l}{v}$.

Figure 1.10 shows the oscillation of the rear of a vehicle with $\alpha = 1$ and shows that in this case the oscillation of the front wheel, which has already started τ seconds ago, does not affect the oscillation of the rear part. That is a result of locating the vibration nodes of the vehicle at the rear and front springs, respectively, the condition for uncoupling.

However, considering Figs. 1.7 and 1.13 for values $\alpha > 1$ and $\alpha < 1$, respectively, the effect of the front oscillation on the rear, is observable in the form of small amplitude oscillations. The time lag oscillation in Fig. 1.7 starts off in the

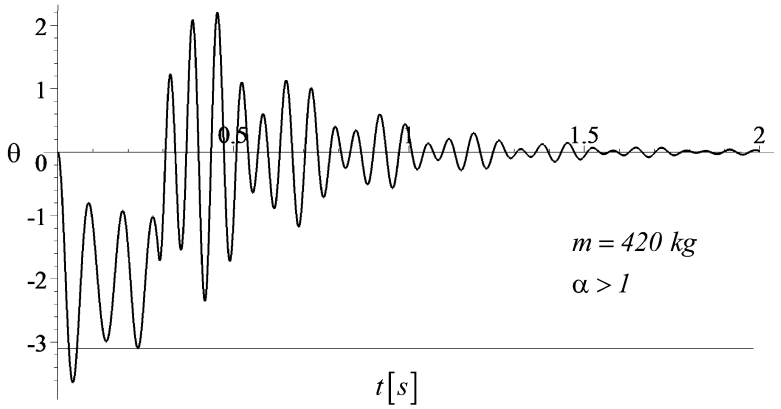

Fig. 1.14 Case 3: angular oscillations of the car with $\alpha < 1$

form of an upward motion which indicates that the oscillation node of the front wheel is located behind the rear wheel having $\alpha > 1$. The condition of the car is reverse for the values of $\alpha < 1$ in Fig. 1.13.

The same conclusions arises by comparing the set of figures which illustrate the pitch motion in the vehicles after hitting the step, Figs. 1.8, 1.11, and 1.14. The angle between the front and rear of the vehicle has been calculated and plotted by:

$$\theta = \frac{x_2 - x_1}{l} \tag{1.30}$$

Smaller pitch motion in Fig. 1.11 for $\alpha = 1$ makes it obvious that an uncoupled system provides a more comfortable ride compared to the pitch angle oscillation θ, in Figs. 1.8 and 1.14.

1.3 No Flat Ride Solution for Linear Suspension

The time lag between the front and rear suspension oscillations is a function of the wheelbase, l, and speed of the vehicle, v. Soon after the rear wheels have passed over a step, the vehicle is at the worst condition of pitching. Olley experimentally determined a recommendation for the optimum frequency ratio of the front and rear ends of cars. His suggestion for American cars and roads of 1950s was to have the natural frequency of the front approximately 80% of that of the rear suspension.

To examine Olley's experimental recommendation and possibly make an analytical base for flat ride, let us rewrite the equation of motion (1.25) and (1.26) as:

$$\ddot{x}_1 + 2\xi_1\dot{x}_1 + \frac{k_1}{m(1-\varepsilon)}x_1 = 2\xi_1\dot{y}_1 + \frac{k_1}{m(1-\varepsilon)}y_1 \tag{1.31}$$

$$\ddot{x}_2 + 2\xi\xi_1\dot{x}_2 + \frac{kk_1}{m\varepsilon}x_2 = 2\xi\xi_1 y_2 + \frac{kk_1}{m\varepsilon}y_2 \tag{1.32}$$

where

$$\xi = \frac{\xi_2}{\xi_1} = \frac{c_1}{c_2}\frac{\varepsilon}{1-\varepsilon} \tag{1.33}$$

$$k = \frac{k_2}{k_1} = \frac{k_1}{k_2}\frac{\varepsilon}{1-\varepsilon} \tag{1.34}$$

$$\xi_1 = \frac{c_1}{m(1-\varepsilon)} \tag{1.35}$$

$$\xi_2 = \frac{c_2}{m\varepsilon} \tag{1.36}$$

Parameters k and ξ are the ratio of the rear/front spring rates and damping ratios, respectively.

The necessity to achieve a flat ride provides that the rear system must oscillate faster to catch up with the front system at a reasonable time. At the time both systems must be at the same amplitude and oscillate together afterwards. Therefore, an ideal flat ride happens if the frequency of the rear system be higher than the front to catch up with the oscillation of the front at a certain time and amplitude. Then, the frequency of the rear must reduce to the value of the front frequency to oscillate in phase with the front. Furthermore, the damping ratio of the rear must also change to keep the same amplitude. Such a dual behavior is not achievable with any linear suspension. Therefore, theoretically, it is impossible to design linear suspensions to provide a flat ride, as the linearity of the front and rear suspensions keep their frequency of oscillation constant.

1.4 Near Flat Ride Solution for Linear Suspensions

To design the rear suspension parameters for a given set of front parameters to achieve a reasonable flat ride condition, we rephrase the problem by introducing a near flat ride condition. The rear suspension must have proper parameters and higher frequency to reach the same amplitude as the front suspension at a reasonable time before the oscillations die out. This brings the vehicle in a flat condition. Then the oscillation of the system dies out before the pitch mode significantly appears again. A near flat ride situation is shown in Fig. 1.15, for a car going over a unit step.

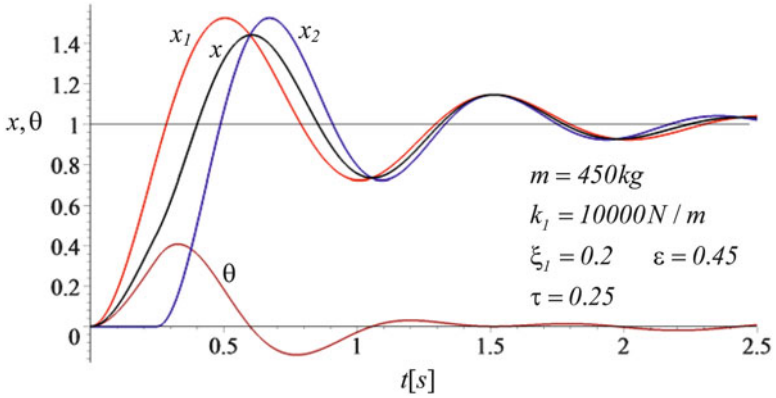

Fig. 1.15 Response of the front and rear suspensions of a near at ride car to a unit step

Solving the equations of motion (1.31) and (1.32) for x_1 and x_2 for a unit step input yields

$$x_1 = 1 - e^{\frac{-\xi_1 \omega t}{\sqrt{1-\varepsilon}}}\left(\cos\sqrt{\frac{1-\xi_1^2}{1-\varepsilon}}\omega t + \frac{\xi_1}{\sqrt{1-\xi_1^2}}\sin\sqrt{\frac{1-\xi_1^2}{1-\varepsilon}}\omega t\right) \tag{1.37}$$

$$t \geq 0$$

$$x_2 = \begin{cases} 0 & t < 0 \\ 1 - e^{-\xi\xi_1\sqrt{\frac{k}{\varepsilon}}(t-\tau)}\left(\cos\sqrt{\frac{k(1-\xi^2\xi_1^2)}{\varepsilon}}\omega(t-\tau)\right. & \\ \left. \quad + \frac{\xi\xi_1}{\sqrt{1-\xi^2\xi_1^2}}\sin\sqrt{\frac{k(1-\xi^2\xi_1^2)}{\varepsilon}}\omega(t-\tau)\right) & t \geq 0 \end{cases} \tag{1.38}$$

where

$$\omega = \sqrt{\frac{k_1}{m}} \tag{1.39}$$

$$\tau = \frac{l}{v} \tag{1.40}$$

As a reasonable catch up time, we search for the conditions such that both systems reach their third equal peak amplitude at the same time.

The third peak of x_1 happens at the time:

$$t_{p_1} = \frac{3\pi\sqrt{1-\varepsilon}}{\omega\sqrt{1-\xi_1^2}} \tag{1.41}$$

where its displacement is:

$$x_1 = 1 + exp(\frac{-3\pi\xi_1}{\sqrt{1-\xi_1^2}}) \tag{1.42}$$

The third peak of x_2 happens at

$$t_{p_2} = \tau + \frac{3\pi\sqrt{\frac{k}{\varepsilon}}}{\omega\sqrt{1-\xi^2\xi_1^2}} \tag{1.43}$$

where its displacement is

$$x_2 = 1 + exp(\frac{-3\pi\xi\xi_1}{\sqrt{1-\xi^2\xi_1^2}}). \tag{1.44}$$

The conditions that x_1 and x_2 meet after one and a half oscillations are:

$$x_1 = x_2 \tag{1.45}$$

$$t_{p_1} = t_{p_2} \tag{1.46}$$

which yield:

$$1 + exp(\frac{-3\pi\xi_1}{\sqrt{1-\xi_1^2}}) = 1 + exp(\frac{-3\pi\xi\xi_1}{\sqrt{1-\xi^2\xi_1^2}}) \tag{1.47}$$

$$\frac{3\pi\sqrt{1-\varepsilon}}{\omega\sqrt{1-\xi_1^2}} = \tau + \frac{3\pi\sqrt{\frac{k}{\varepsilon}}}{\omega\sqrt{1-\xi^2\xi_1^2}}. \tag{1.48}$$

Equation (1.47) is independent of the spring ratio k and can be solved for damping ratio ξ

$$\xi = 1. \tag{1.49}$$

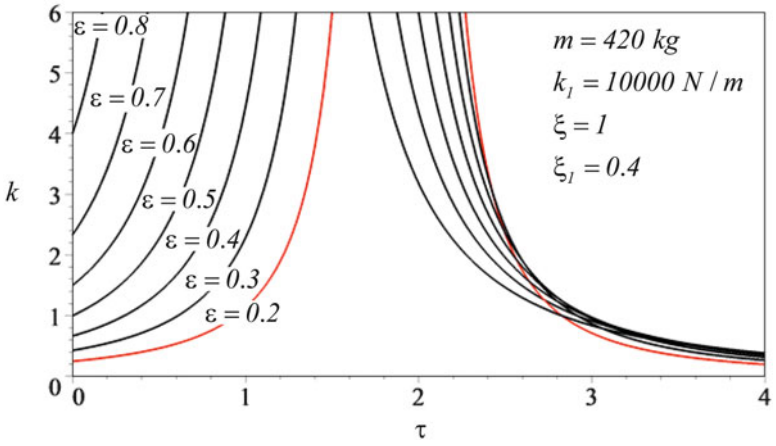

Fig. 1.16 Illustrates the plot of k versus τ, for different ε from 0.2 to 0.8

It indicates that the third peak of the motion of the front and rear of the car will be equal provided the damping coefficient of the front and rear suspensions are equal.

Solving (1.48) for spring ratio k yields:

$$k = \frac{Z_1}{Z_2\tau^2 + Z_3\tau + Z_4} \tag{1.50}$$

where

$$Z_1 = -9\varepsilon\pi^2 m(-1 + \xi_1^2) \tag{1.51}$$

$$Z_2 = (\xi^2\xi_1^4 - \xi^2\xi_1^2 + 1 - \xi_1^2)k_1 \tag{1.52}$$

$$Z_3 = 6\pi m(\xi^2\xi_1^2 - \varepsilon\xi^2\xi_1^2 - 1 + \varepsilon)\sqrt{-\frac{k_1(1-\xi_1^2)}{m(\varepsilon-1)}} \tag{1.53}$$

$$Z_4 = -9\pi^2 m(\varepsilon\xi^2\xi_1^2 - \varepsilon + 1 - \xi^2\xi_1^2) \tag{1.54}$$

Using a set of nominal values,

$$\xi = 1 \qquad m = 420 \qquad \xi_1 = 0.4 \qquad k_1 = 10000. \tag{1.55}$$

Figure 1.16 illustrates the plot of k versus τ, for different ε from 0.2 to 0.8. Using this graph, we can determine the value of spring ratio k for a given $\varepsilon = a_1/l$ and $\tau = l/v$. Because for a given car, the values of ε and l are fixed, the graph determines the required $k = k_2/k_1$ at any speed v.

Considering the existing designs of normal street vehicles, only a very small section of the horizontal axis of Fig. 1.16 should be investigated. The wheelbase

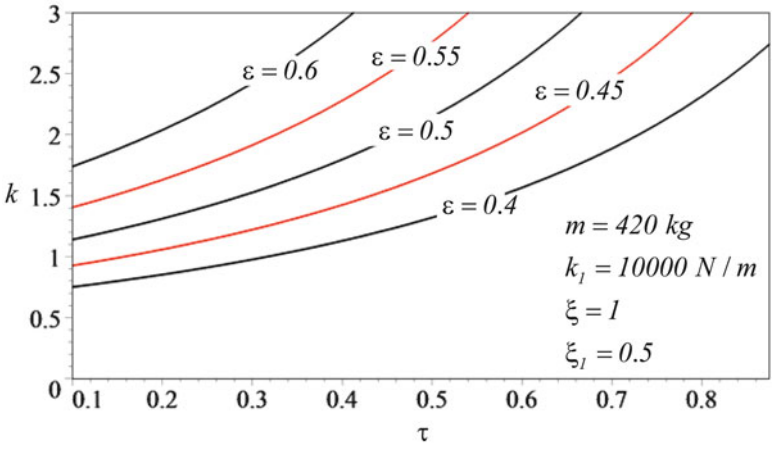

Fig. 1.17 Plots of k versus τ for $\xi_1 = 0.5$ and different ε in the domain $0.1 < \tau < 0.875$

for normal street vehicles is usually not less than 2 m or longer than 3.5 m. Let us assume that the speed of a car which goes over a step and is expected to show a flat ride, is between 4 and 20 m/s. Therefore, the practical domain of the time lag between the front and rear wheels would be $0.1 < \tau < 0.875$.

Furthermore, the mass center of street cars are normally in the front half of the wheelbase in order to provide understeer condition. Considering $0.4 < \varepsilon < 0.6$ will cover all street and sports cars. Figure 1.17 shows how k varies with τ for $\xi_1 = 0.5$ and different ε to provide a near flat ride. For any ε, the required stiffness ratio increases by increasing τ. Therefore, the ratio of rear to front stuffiness increases when the speed of the car decreases. It is because the frequency of the rear part must be higher to catch up with the oscillations of the front. Figure 1.18 illustrates the same information in the plane of (ε, τ). It shows that for a constant k, how the mass center of a car should change to provide a near flat ride. The value of ε is a decreasing function of τ and therefore, the mass center of a car should get closer to the front axle when the speed of the car increases. Ideally, the curves in both Figs. 1.17 and 1.18 must be horizontal to have a constant stiffness ratio to achieve a near flat ride at any speed. However, not only a flat ride is impossible to achieve, a near flat ride also is not achievable by linear suspensions.

Figures 1.19–1.26 depict the similar information of Figs. 1.17 and 1.18 for $\xi_1 = 0.4$, $\xi_1 = 0.3$, $\xi_1 = 0.2$, and $\xi_1 = 0.1$, respectively.

Let us consider having a vehicle with smart suspension, and the effect of change of traveling speed of the vehicle on the near flat ride, Figs. 1.18, 1.20, 1.22, 1.24, and 1.26 can be used as design charts. As an example, the average length of a sedan vehicle has been taken equal to 2.6 m with a normal weight distribution of a front differential vehicle 56/44 heavier at the front. Using the given information some other values can be calculated as: $a_1 = 1,144$ mm and $a_2 = 1,456$ mm which yields to $\varepsilon = 0.44$. Assuming that the front suspension of the car has a damping of

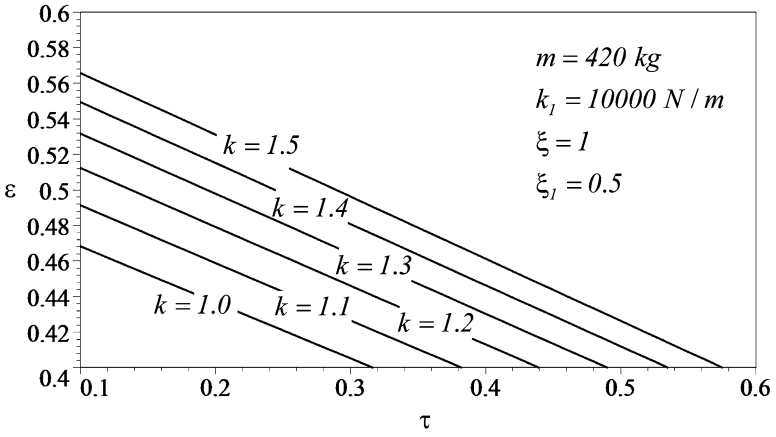

Fig. 1.18 τ versus ε for different spring rates

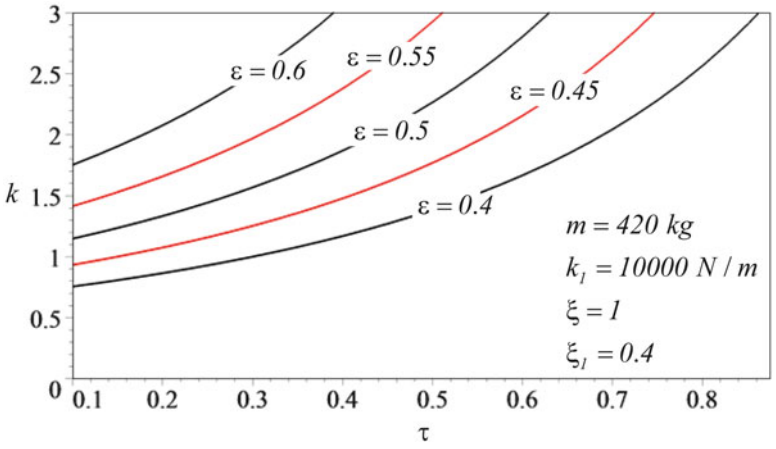

Fig. 1.19 Plots of k versus τ for $\xi_1 = 0.4$ and different ε in the domain $0.1 < \tau < 0.875$

$\xi_1 = 0.4$, the diagram in Fig. 1.20 can be used by the smart suspension to provide near flat ride in different speeds, by switching the spring rate to the required value. Continuous variation of k is illustrated in Fig. 1.21. The horizontal line in Fig. 1.27 is showing the values that the spring should be switching to as the traveling speed of the vehicle on the example changes, which is the ideal situation for near flat ride. To use the same chart for vehicles with passive suspension, a target speed needs to be chosen by the designer as the ideal speed for the vehicle to have a near flat ride. The point in Fig. 1.27 is indicating that for a car with passive suspension, with a wheelbase of 2.4 m, traveling speed of 29 km/h, to get a near flat ride a spring ratio of $k = 1.2$ is needed.

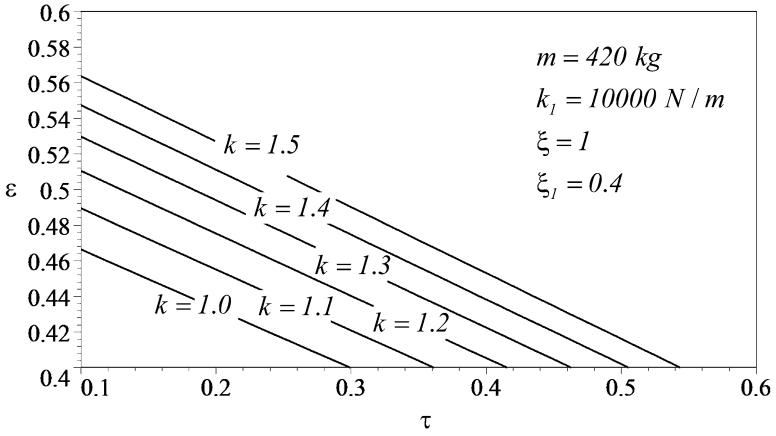

Fig. 1.20 τ versus ε for different spring rates for $\xi = 0.4$

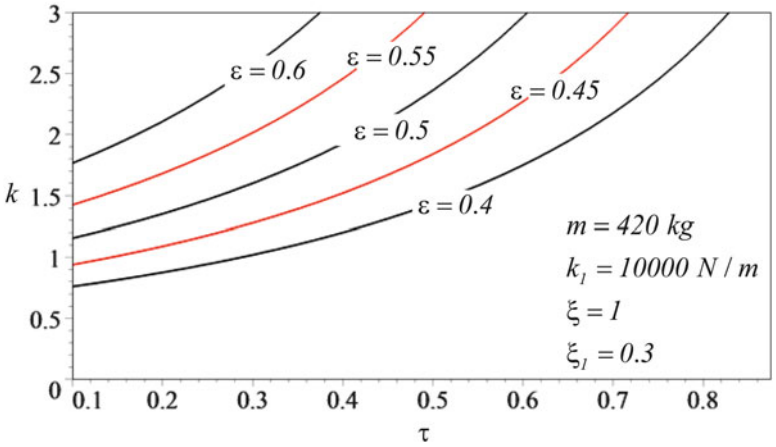

Fig. 1.21 Plots of k versus τ for $\xi_1 = 0.3$ and different ε in the domain $0.1 < \tau < 0.875$

1.5 Nonlinear Damper

The force–velocity characteristics of an actual shock absorber can be quite complex as is shown in Fig. 1.28. Although we may express the complex behavior using an approximate function, analytic calculation can be quite complicated with little design information. Furthermore, the representations of the exact shock absorber do not greatly affect the behavior of the system. The simplest linear viscous damper model is usually used for linear analytical calculation

$$F_D = cv_D, \tag{1.56}$$

where c is the damping coefficient of the damper.

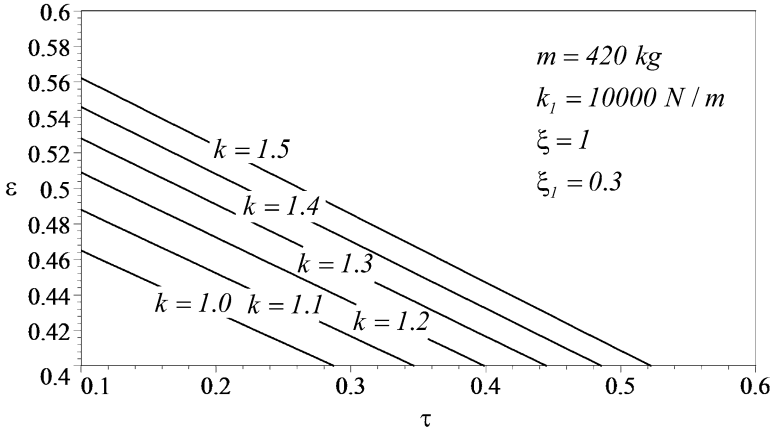

Fig. 1.22 τ versus ε for different spring rates for $\xi = 0.3$

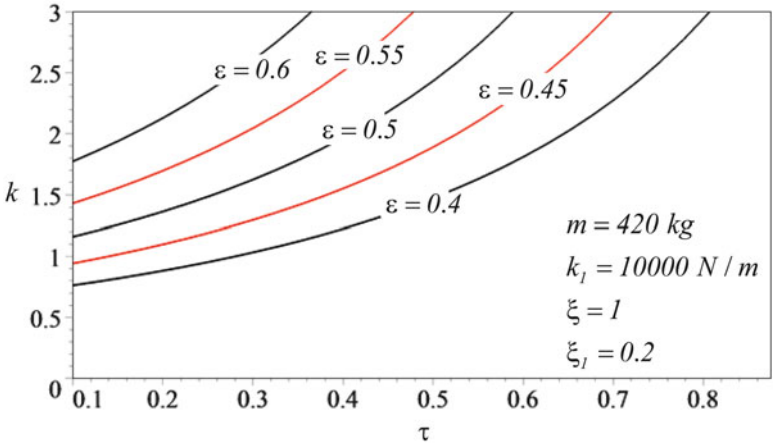

Fig. 1.23 Plots of k versus τ for $\xi_1 = 0.2$ and different ε in the domain $0.1 < \tau < 0.875$

As seen in Fig. 1.28 the bound and rebound forces of the damper are different, in other words the force–velocity characteristics diagram is not symmetric. Practically, a shock absorber compresses much easier than decompression. A reason is that during rebound in which the damper extends back, it uses up the stored energy in the spring. A high compression damping prevents to have enough spring compression to collect enough potential energy. That is why in order to get a more reliable and close to reality response for analysis on dampers, using bilinear dampers are suggested. It is similar to a linear damper but with different coefficients for the two directions [3]. The behavior of such damper models is illustrated in Fig. 1.29

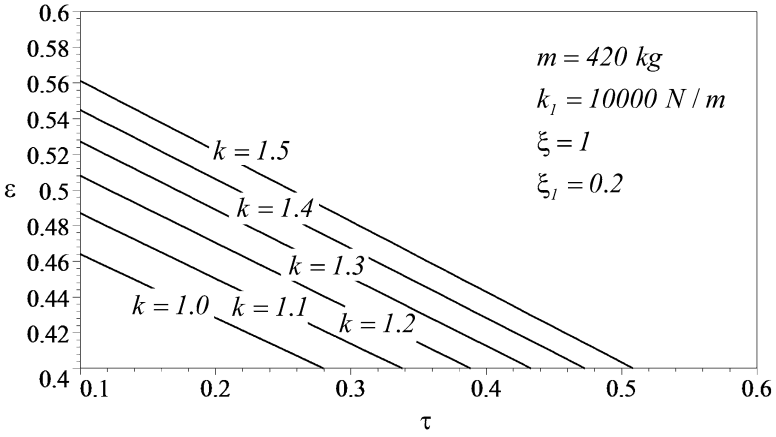

Fig. 1.24 τ versus ε for different spring rates for $\xi = 0.2$

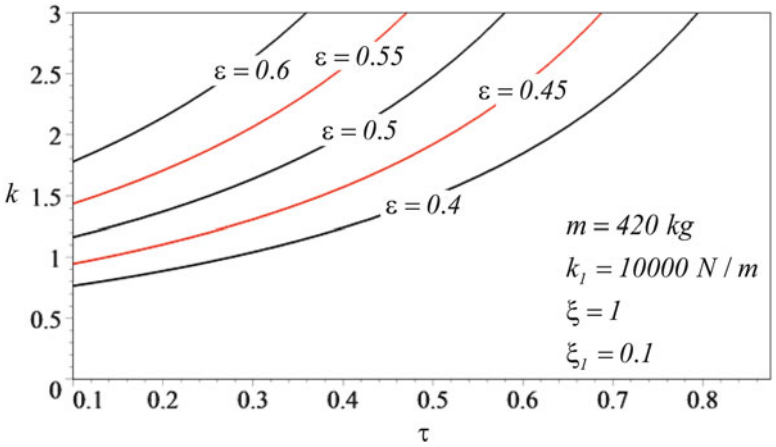

Fig. 1.25 Plots of k versus τ for $\xi_1 = 0.1$ and different ε in the domain $0.1 < \tau < 0.875$

$$F_D = \begin{cases} c_{DE} v_D & Extension \\ c_{DC} v_D & Compression \end{cases} \tag{1.57}$$

where c_{DE} is the damping coefficient when damper is extended and c_{DC} is the damping coefficient when the damper is compressed.

An ideal dual behavior damper is one which does not provide any damping while being compressed and, on the other hand, damps the motion while extending. Based on this model, the nonlinear damper model's behavior used for this study is illustrated in Fig. 1.30. Using the nonlinear damper model and following the same steps as the previous section, we can compare two systems to determine the effectiveness of damping on the flat ride.

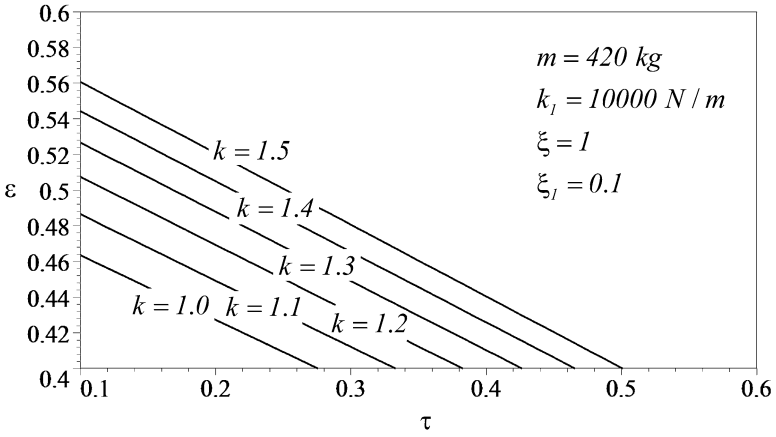

Fig. 1.26 τ versus ε for different spring rates for $\xi = 0.1$

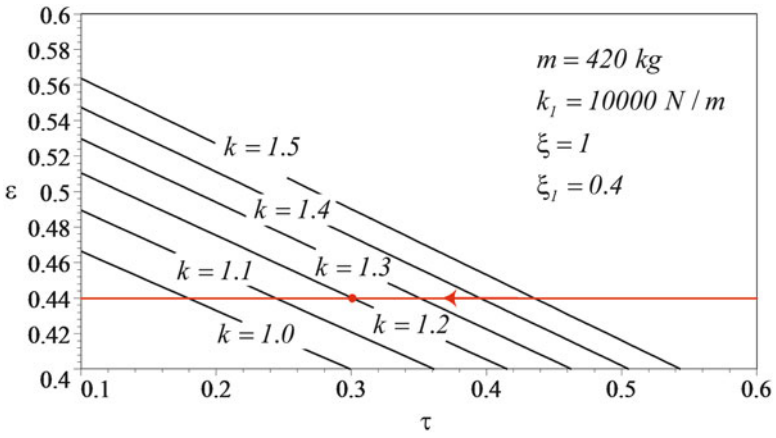

Fig. 1.27 Design chart for a smart suspension with a linear damper

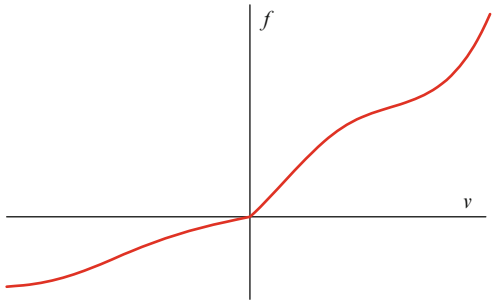

Fig. 1.28 The force–velocity characteristics of a real damper

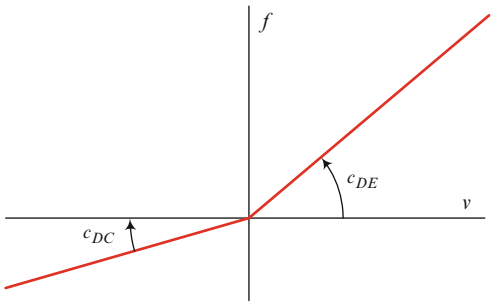

Fig. 1.29 Force–velocity characteristics of a bilinear damper

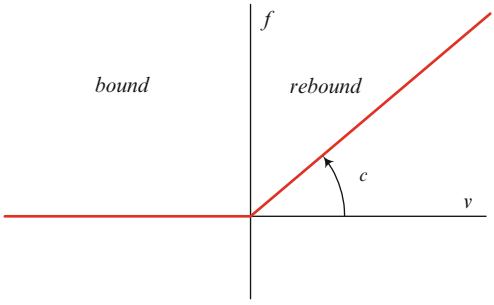

Fig. 1.30 Force–velocity characteristic of an ideal nonlinear damper model

Equations (1.37) and (1.38) have been used to get the motion of the front and rear of the vehicle after hitting a unit step. The only difference is that the motion is investigated in three steps for the front and same for the rear. Ideally, the unit step moves the ground up in no time and therefore the motion of the system begins when $y = 1$ and the suspension is compressed. The first step is right after the wheel hits the step and the damper starts extending which means the positive side of Fig. 1.30 would be in action. The second step is when the damper starts the compression phase, and according to the figure the damping coefficient would be equal to zero. The third step is when the damper starts extending again. Each of (1.37) and (1.38) should be solved for the three steps separately in order to find the time and amplitude of the third peak of the motion.

Figure 1.31 illustrates the behavior of the car equipped with a nonlinear damper when going over a unit step input. Figure 1.32 also illustrates the behavior of the same car if the damper was linear. Comparison of the behavior of the car for linear and nonlinear dampers is plotted in Figs. 1.33 and 1.34 for front and rear suspensions, respectively. The linear damper dissipates energy in both, bound and rebound cycles, while the nonlinear damper dissipates energy only in rebound cycle. Therefore, the linear damper is more effective in energy dissipation and damps the system faster. This fact can be seen in both Figs. 1.33 and 1.34.

To compare the behavior of a car with both cycle linear damper and one cycle nonlinear damper, we also analyze the opposite cycle nonlinear damper of Fig. 1.35. The response of the car to the opposite cycle nonlinear damper is illustrated in Fig. 1.36. Comparison of the linear and nonlinear dampers for the front and rear suspensions is plotted in Figs. 1.37 and 1.38, respectively.

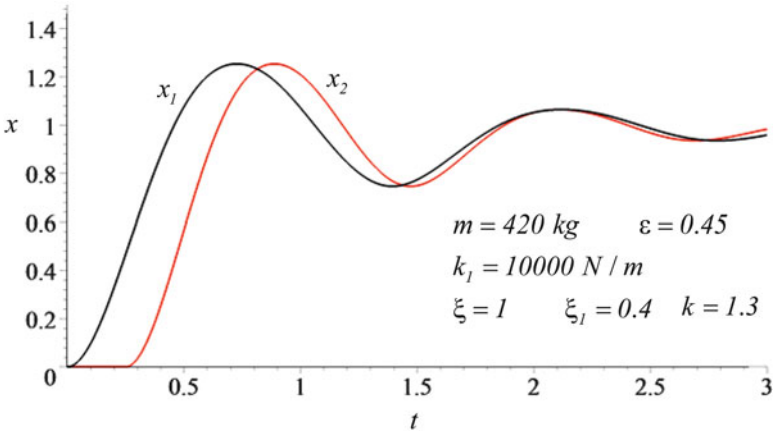

Fig. 1.31 Response of the front and rear suspensions of a near flat ride car with ideal nonlinear damper to a unit step

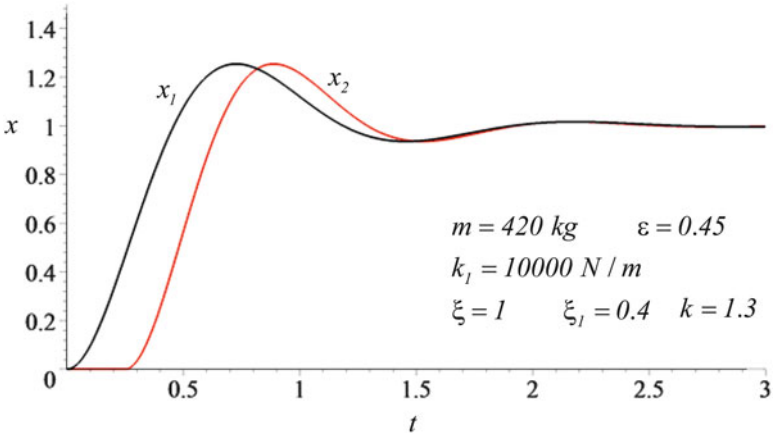

Fig. 1.32 Response of the front and rear suspensions of a car with linear damper to a unit step

1.6 Near Flat Ride Solution for Ideal, Nonlinear Damper

The conditions that x_1 and x_2 meet after one and a half oscillations are the same as (1.45) and (1.46). The equation resulted from $x_1 = x_2$ has got ξ and ξ_1 as its variables and could be plotted as an explicit function of the variables which interestingly shows that the value for $\xi = \xi_2/\xi_1$ must equal to 1 for any value for damping coefficient of the front suspension. Therefore, regardless of the value of ξ_1 the rear suspension should have an equal coefficient for the damper. The equation resulted from $t_{P_1} = t_{p_2}$ generates an equation to determine $k = k_2/k_1$. Figure 1.39

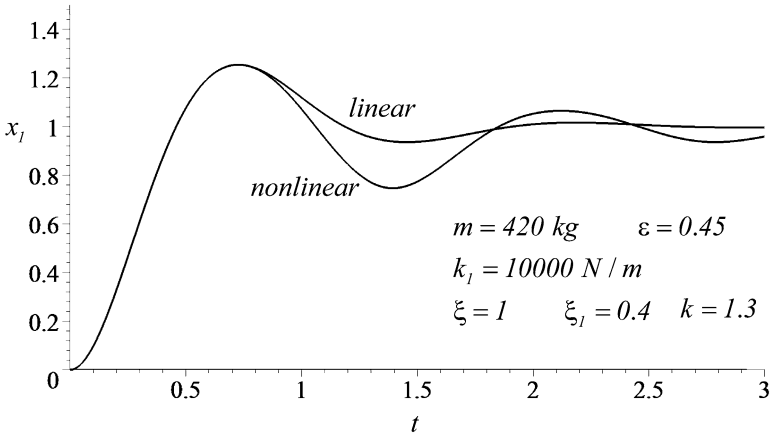

Fig. 1.33 Comparison of the behavior of the front suspensions of the car for linear and nonlinear dampers

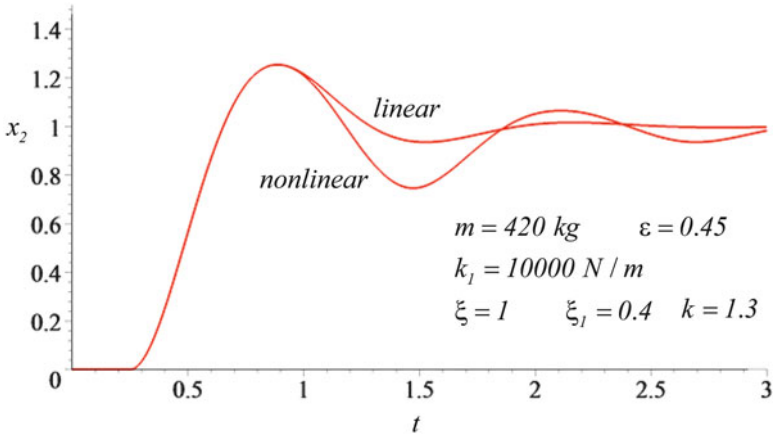

Fig. 1.34 Comparison of the behavior of the rear suspensions of the car for linear and nonlinear dampers

illustrates the spring ratio $k = k_2/k_1$ versus $\tau = l/v$, to have near flat ride with ideal nonlinear damping, for different $\varepsilon = a_1/l$.

Once again, considering the existing designs street vehicles, only the small section of $0.1 < \tau < 0.875$ of Fig. 1.39 is applied. The mass center of street cars is also limited to $0.4 < \varepsilon < 0.6$.

Figure 1.40 shows how k varies with τ for $\xi_1 = 0.5$ and different ε to provide a near flat ride with ideal nonlinear damper. For any ε, the required stiffness ratio increases by increasing τ. Therefore, the ratio of rear to front stuffiness increases when the speed of the car decreases. Figures 1.41–1.44 also provide the same design graphs for $\xi_1 = 0.4, 0.3, 0.2, 0.1$, respectively.

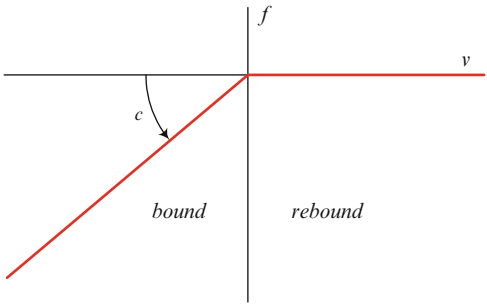

Fig. 1.35 Force–velocity characteristic of an opposite cycle nonlinear damper model

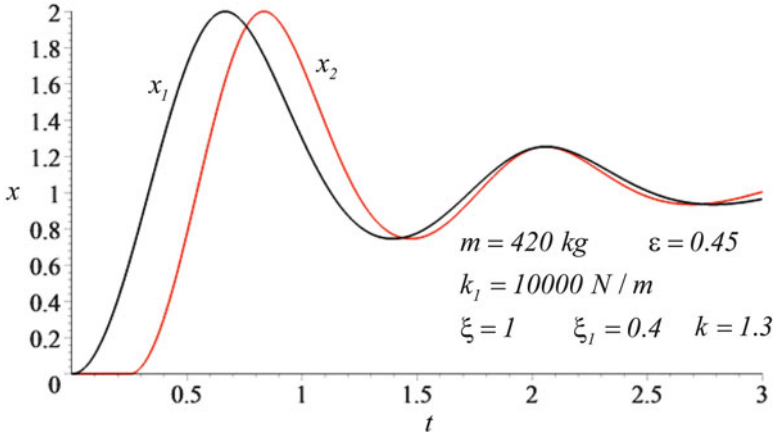

Fig. 1.36 Response of the front and rear suspensions of a near flat ride car with ideal nonlinear damper to a unit step

Using a nonlinear damper for studying Olley's flat ride tuning shows the same behavior as a linear damper. So, the same trend as for the linear case can be taken here. There will be a possibility of using the τ versus ε diagrams as a design chart.

1.7 The First Investigations

Maurice Olley was one of the first pioneers who introduced and studied the concept of flat ride in vehicle dynamics. He was an English engineer born in 1889, who during his life added a lot to the general knowledge of vehicle dynamics and is counted as one of the great automobile engineers of his era. He is one of the founders of modern vehicle dynamics. In his early career in the Rolls Royce design office, he worked under Sir Henry Royce but the majority of his career was spent at Cadillac in the USA and Vauxhall in England.

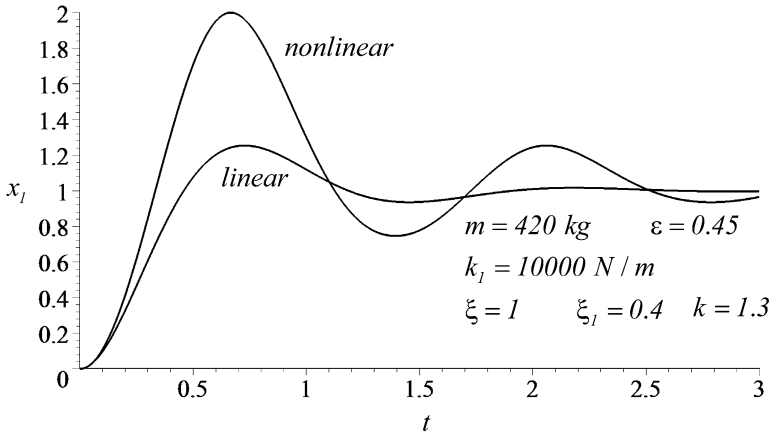

Fig. 1.37 Comparison of the behavior of the front suspensions of the car for linear and opposite cycle nonlinear dampers

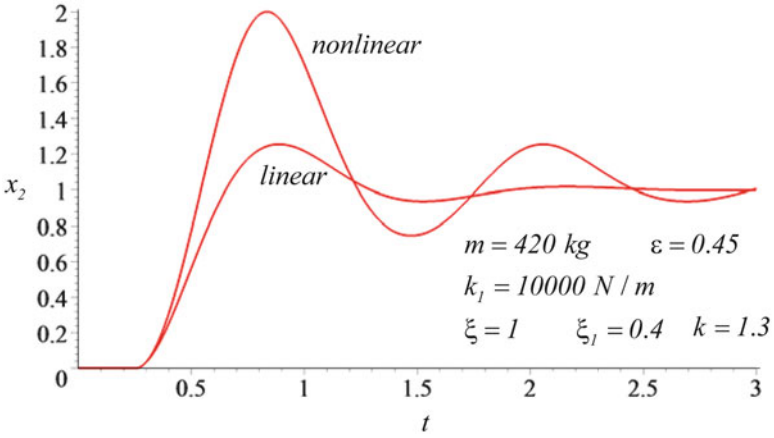

Fig. 1.38 Comparison of the behavior of the rear suspensions of the car for linear and opposite cycle nonlinear dampers

Olley worked directly for Sir Henry Royce and was in the United States for some 10 years struggling to get off the ground the manufacture of Rolls-Royce cars at Springfield, Massachusetts. The financial crash of 1929 put the skids under the operation. His first task after moving to the Cadillac company in 1930 was suspension and ride. He introduced the Rolls-Royce type of bump rig and began a full program of ride development. He studied the oscillation of wheels and tires and by applying some changes on the rig was soon studying the basic ride motions of the car. In his paper [6] he published the results taken from his experiments using the test rig for the first time.

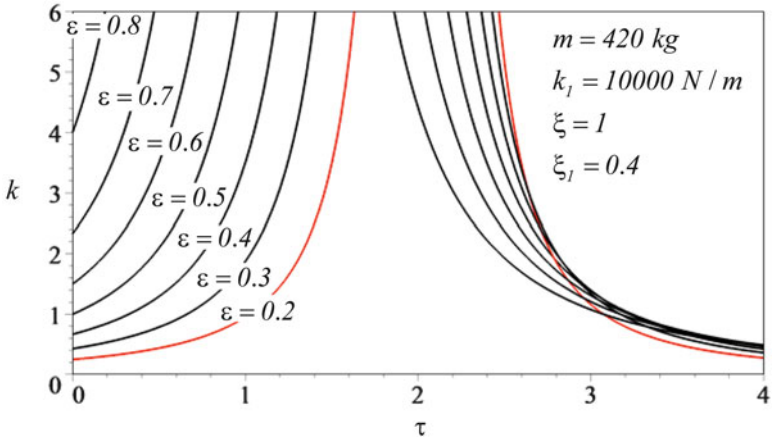

Fig. 1.39 The value of spring ratio $k = k_2/k_1$ versus $\tau = l/v$, to have near flat ride with ideal nonlinear damping, for different $\varepsilon = a_1/l$

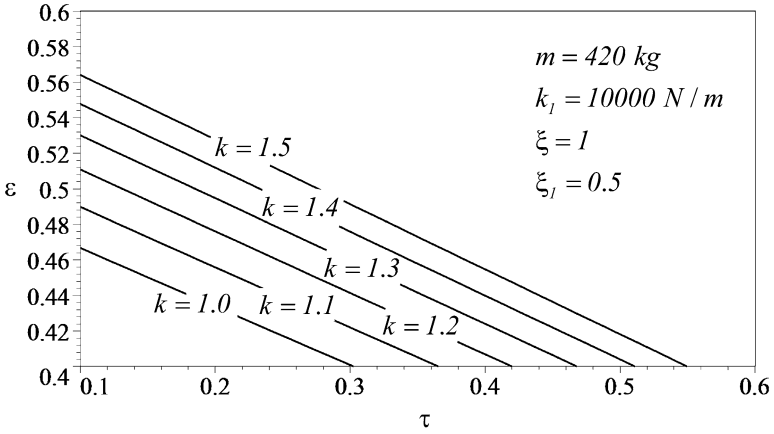

Fig. 1.40 ε versus τ, for different k for $\xi_1 = 0.5$ to have near flat ride with ideal nonlinear damping

He developed a bouncing table rig in General Motors proving grounds, on which humans were vibrated vertically at different frequencies and amplitudes. They would have increased the frequency till the person on the table begins to feel uncomfortable. Using this equipment Olley explained the relation between vertical acceleration and comfort over a range of frequencies. He generated a curve for passenger comfort, which is very similar to the current ISO2631 standard.

Olley as well as other investigators in well-established car companies realized that the pitch and roll modes of the car body are much more uncomfortable than the bounce mode. The investigators' effort focused on the suspension stiffness and damping rates to be experimentally adjusted to provide acceptable vertical

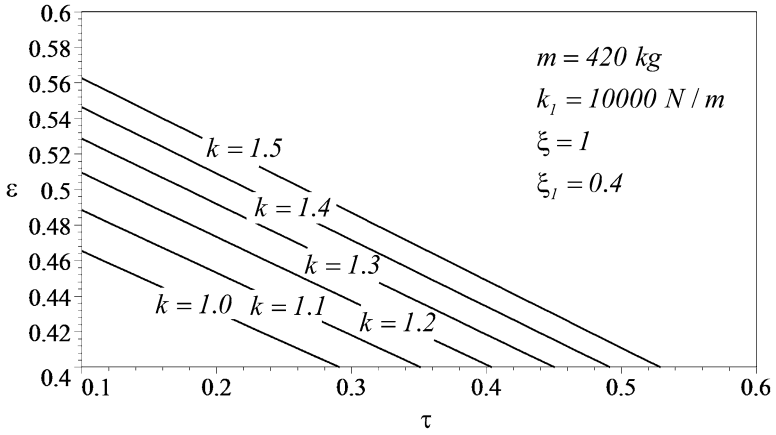

Fig. 1.41 ε versus τ, for different k for $\xi_1 = 0.4$ to have near flat ride with ideal nonlinear damping

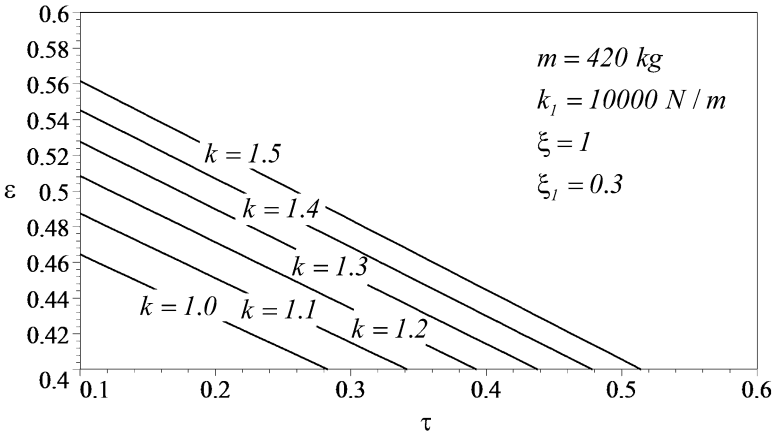

Fig. 1.42 ε versus τ, for different k for $\xi_1 = 0.3$ to have near flat ride with ideal nonlinear damping

vibrations. However, the strategy about roll and pitch modes was to transform them to bounce. Due to usual geometric symmetry of cars, as well as the symmetric excitation from the road, roll mode is being excited much less than pitch mode. Therefore, lots of investigations have been focused on adjustment of the front and rear suspensions such that pitch mode of vibration transform to the bounce.

In the early 1930s most cars were built with fairly stiff springs at the front and soft at the rear, with a $\frac{r^2}{a_1 a_2}$ ratio in pitch of about 0.8, where r is the pitch radius of gyration of the car and a_1 and a_2 are the distance of the mass center, C, from the front and rear axles, as shown in Fig. 1.45 [1]. However, based on what Olley discovered, such a choice was against the mode transfer desire.

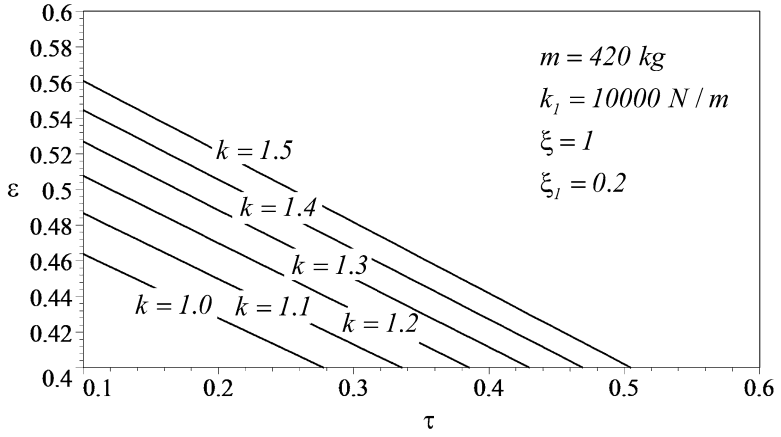

Fig. 1.43 ε versus τ, for different k for $\xi_1 = 0.2$ to have near flat ride with ideal nonlinear damping

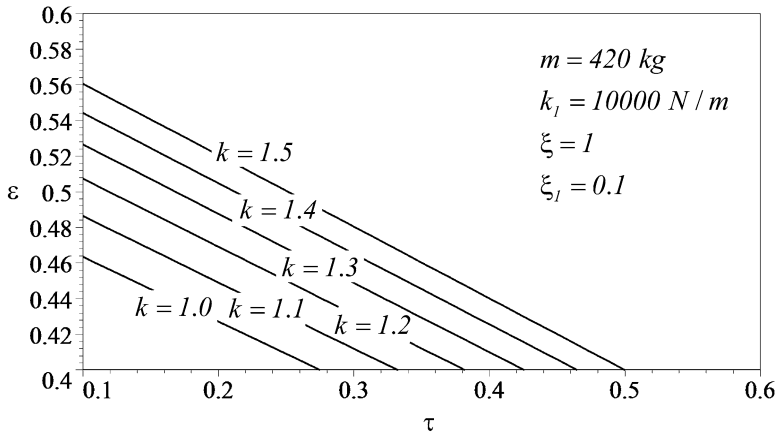

Fig. 1.44 ε versus τ, for different k for $\xi_1 = 0.1$ to have near flat ride with ideal nonlinear damping

Besides all the important facts that Olley discovered during his experiments, the principle known as the flat ride tuning or Olley's flat ride proved to be more industry approved and accepted. After his publications [6–8] in which he advocated this design practice, they became rules of practice.

We can summarize what has been said about ride and comfort in American passenger cars by Olley as the following:

1. The front spring should be softer than the rear for flat ride tuning. This will promote bouncing of the body rather than pitching motions at least for a greater majority of speeds and bump road situations. The front suspension should have

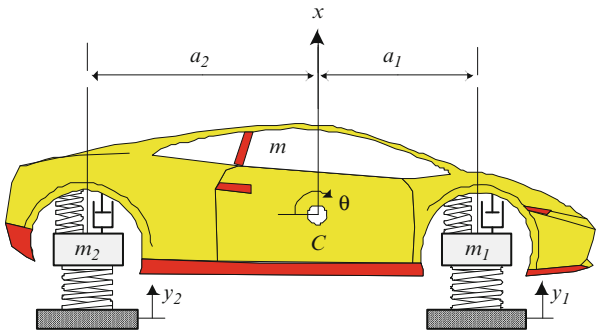

Fig. 1.45 Bicycle car model used for analyzing vibrations

a 30% lower ride rate than the rear suspension, or the spring center should be at least 6.5% of the wheelbase behind the center of gravity. Although this does not explicitly determine the front and rear natural frequencies, since the front-rear weight distribution on passenger cars is close to 50–50, it will generally assure that the rear frequency is greater than the front.

2. The ratio $\frac{r^2}{a_1.a_2}$ normally approaches unity. This reduces vibration interactions between front and rear because the two suspensions can now be considered as two separate systems. As a consequence there will be less resonant build-ups on the road and the pitching frequency will have a magnitude closer to that of bounce.
3. The pitch and bounce frequencies should be close together: the bounce frequency should be less than 1.2 times the pitch frequency. For higher ratios interference kicks resulting from the superposition of the two motions. This condition will be met for modern cars because the dynamic index is near unity with the wheels located near the forward and rearward extremes of the chassis.
4. Neither frequency should be greater than 1.3 Hz, which means that the effective static deflection of the vehicle should exceed roughly 6 in.
5. The roll frequency should be approximately equal to the pitch and bounce frequencies. To minimize roll vibrations the natural frequency in roll needs to be low just as for the bounce and pitch modes.

Rowell and Guest [9] in 1923 identified the value of $\frac{r^2}{a_1.a_2}$ being associated with vehicles in which the front and rear responses were uncoupled. Olley was able to investigate the issue experimentally and these experiments led him to the belief that pitching motion was extremely important in the subjective assessment of vehicle ride comfort. He built the Cadillac k_2 rig in 1931 which was a 12 cylinder, 7 passenger Cadillac limousine of the period, fitted with front and rear outriggers each of which could carry up to 327 kg made up in 27 kg weights. To their surprise, under these supposedly ideal conditions, they still got an unsatisfactory ride. This arrangement gave no fixed oscillation centers and the ride had no pattern. However, by fitting all the weights they found that if the front spring static deflections are some 30% greater than the rear, then the revolutionary flat ride occurs. Olley's explanation

was that because the two ends of the car did not cross a given disturbance at the same instant it was important that the front wheels initiated the slower mode and that the rear wheels initiated the faster mode. This allowed the body movement at the rear to catch up the front and so produce the flat ride.

The condition of Flat Ride is expressed in various detailed forms; however, the main idea states that *the front suspension should have a 30% lower ride rate then the rear.* The physical explanation for why this is beneficial in reducing pitch motion is usually argued based on the time history of events following a vehicle hitting a bump. First, the front of the vehicle responds "approximately in the well-known damped oscillation manner." At some time later, controlled by the wheelbase and the vehicle speed, the rear responds in similar fashion. The net motion of the vehicle is then crudely some summation of these two motions which minimizes the vehicle pitch response [2].

Confirmation of the effectiveness in pitch reduction of the Olley design was given by Best [1] over a limited range of circumstances. Random road excitation was applied to a half-car computer model, with identical front and rear excitations, considering the time delay generated by the wheelbase and vehicle's speed. Pitch suppression was associated with the wheelbase filtering effect. Pitch suppression appeared to be necessarily associated with increases in bounce response, leaving in unclear whether or not it is a worthwhile goal [10].

Sharp and Pilbeam [11] attempted a more fundamental investigation of the phenomenon, primarily by calculating frequency response for the half-car over a wide range of speed and design conditions. At higher speeds, remarkable reductions in pitch response with only small costs in terms of bounce response were shown. At low speeds, the situation is reversed. These behavioral features were shown to be generic insofar as variations in mass center location, pitch inertia and damping level were concerned, and the implications from the frequency responses were confirmed by simulations with nonlinear asymmetric suspension damping.

Later on Sharp [10] discussed the rear to front stiffness tuning of the suspension system of a car, through reference to a half-car pitch plane mathematical model. He used new results relating to the frequency responses of the bouncing and pitching motions of the car body to show that the pitch minimization mechanism of Olley's flat ride tuning "involves interference between the responses to the front and rear axle inputs." He showed that interference with respect to the rotational motion implies reinforcement with respect to the translational motion, and vice versa. Sharp concludes almost the same facts mentioned by Best and other researchers before him, saying that at higher vehicle speeds, Olley tuning is shown to bring advantage in pitch suppression with a very little disadvantage in terms of body acceleration. At lower speeds, he continues, not only does the pitch tuning bring large vertical acceleration penalties but also suspension stiffness implied are impractical from an attitude control standpoint.

The flat ride problem was revisited by Crolla and King [2]. They generated vehicle vibration response spectra under random road excitations. Some results included the wheelbase filter effect, while others did not. Olley and reverse Olley designs were simulated at speeds of 10, 20, 30, and 40 m/s, with the result that

Olley design was good in pitch and bad in bounce in all cases. It was confidently concluded that the rear/front stiffness ratio has virtually no effect on overall levels of ride comfort.

In 2004, Odhams and Cebon investigated the tuning of a pitch-plane model of a passenger car with a coupled suspension system and compared it to that of a conventional suspension system, which followed the Rowell and Guest treatment [5]. They believed that there is a significant benefit from coupling front and rear suspensions; coupled suspensions with a "Hydrolastic" or "Hydragas" systems, in which the front and rear suspension struts are connected hydraulically, have proved very effective in some applications. The concluded that the Olley's flat ride tuning provides a near optimum stiffness choice for conventional suspensions for minimizing dynamic tire forces and is very close to optimal for minimizing horizontal acceleration at the chest (caused by pitching) but not the vertical acceleration.

Key Symbols

a_1	Distance from the front wheel to the C
a_2	Distance from the rear wheel to the C
c	Damping coefficient
C	Mass center
C_{DC}	Damping coefficient in compression
C_{DE}	Damping coefficient in extension
F_D	Damping force
I	$= mr^2$ mass moment
k	$= k_2/k_1$
k_1	Front spring rate
k_2	Rear spring rate
k_T	Tire stiffness
k_f	Front spring rate
k_r	Rear spring rate
k'_F	Front ride rate
k'_R	Rear ride rate
l	Wheelbase
m	Mass
m_1	Front mass portion
m_2	Rear mass portion
q_1	$= \left(k'_F + k'_R\right)/m$
q_2	$= \left(a_1 k'_F - a_2 k'_R\right)/m$
q_3	$= \left(a_1^2 k'_F + a_2^2 k'_R\right)/I$

r	Radius of gyration
τ	Time lag
t_{p_1}	Time of the third peak of the front
t_{p_2}	Time of the third peak of the rear
u_1	First mode shape of the system
u_2	Second mode shape of the system
v	Velocity of the vehicle
v_D	Vertical velocity of the damper
x_1	Vertical movement of the front wheel
x_2	Vertical movement of the rear wheel
y_1	Road input to the front wheel
y_2	Road input to the rear wheel

Greek

α	$= r^2/a_1a_2$ nondimensional parameter
β	$= l^2/a_1a_2$ nondimensional parameter
γ	Rate to front length ratio
θ	Pitch angle
ε	$= a_1/l$ nondimensional parameter
ξ_1	Front damping ratio
ξ_2	Rear damping ratio
ξ	$= \xi_2/\xi_1$ rear to front damping ratio
η_b	Distance from bounce center to the C
η_p	Distance from pitch center to the C
ω_1	First natural frequency of the system
ω_2	Second natural frequency of the system
Ω_1	$= \sqrt{k_1\beta/m}$ nondimensional parameter
Ω_2	$= \sqrt{k_2\beta/m}$ nondimensional parameter

References

1. Best A (2002) Vehicle ride-stages in comprehension. Phys Technol 15(4):205
2. Crolla D, King R (2000) Olley's "Flat Ride" [revisited]
3. Dixon J (2008) The shock absorber handbook. Wiley, New York
4. Milliken WF, Milliken DL, Olley M (2002) Chassis design. Professional Engineering Publishing, Bury
5. Odhams A, Cebon D (2006) An analysis of ride coupling in automobile suspensions. Proc Inst Mech Eng D J Automob Eng 220(8):1041–1061
6. Olley M (1934) Independent wheel suspension 'its whys and wherefores'. Soc Automot Eng J 34(3):73–81
7. Olley M (1938) National influences on American passenger car design. Proc Inst Automob Eng 32(2):509–572

8. Olley M (1946) Road manners of the modern car. Proc Inst Automob Eng 41(1):147–182
9. Rowell HS, Guest JJ (1923) Proc Inst Automob Eng 18:455
10. Sharp R (2002) Wheelbase filtering and automobile suspension tuning for minimizing motions in pitch. Proc Inst Mech Eng D J Automob Eng 216(12):933–946
11. Sharp R, Pilbeam C (1993) Achievability and value of passive suspension design for minimum pitch response. In: Vehicle Ride and Handling, vol 39, pp 243–259